Available online at www.sciencedirect.com

SciVerse ScienceDirect

journal homepage: www.elsevier.com/locate/jmbbm

Research Paper

Effect of partial crystallization on the mechanical properties and cytotoxicity of bioactive glass from the $3CaO.P_2O_5$–SiO_2–MgO system

J.K.M.F. Daguano[a,*], K. Strecker[b], E.C. Ziemath[c], S.O. Rogero[d], M.H.V. Fernandes[e], C. Santos[f,g]

[a]EEL—USP, Escola de Engenharia de Lorena da Universidade de São Paulo, Polo Urbo-Industrial, Gleba AI-6, s/n, Mondesir, PC 116, Lorena (SP), Brazil
[b]UFSJ—CENEN, Universidade Federal de São João del-Rei, Campus Sto Antônio, Praça Frei Orlando 170, Centro, S. J. del-Rei (MG), Brazil
[c]UNESP, Universidade Estadual Paulista, Departamento de Física, Instituto de Geociências e Ciências Exatas, Rio Claro (SP), Brazil
[d]IPEN/CNEN-SP, Instituto de Pesquisas Energéticas e Nucleares, São Paulo (SP), Brazil
[e]CICECO, Universidade de Aveiro, Aveiro 3810-193, Portugal
[f]UNIFOA—MeMAT, Centro Universitário de Volta Redonda, Pró-Reitoria de Pesquisa e Extensão, V. Redonda (RJ), Brazil
[g]UERJ—FAT, Universidade Estadual do Rio de Janeiro, Departamento de Mecânica e Energia - Rod Presidente Dutra, km 298, Resende (RJ), Brazil

ARTICLE INFO

Article history:
Received 2 February 2012
Received in revised form
26 April 2012
Accepted 30 April 2012
Available online 14 May 2012

Keywords:
Glass-ceramics
Crystallization
Microstructure
Mechanical properties
Cytotoxicity

ABSTRACT

The aim of this study is to report on the development and characterization of bioactive glass and glass-ceramics from the $3CaO.P_2O_5$-SiO_2-MgO-system, using different degrees of cristallinity for applications as an implant material. A methodology was proposed to induce crystallization of phases. Bioglass samples of the nominal composition (wt %) 57.75 $CaO.P_2O_5$–30 SiO_2–17.25 MgO were heat treated at temperatures ranging from 700 to 1100 °C for 4 h. The findings from the research illustrate how partial crystallization and phase transformations modified the microstructure of the based glassy material, resulting in improved mechanical properties. The maximum gain was measured for samples treated at 975 °C, having a hardness of 6.2 GPa, an indentation fracture toughness of 1.7 $MPam^{1/2}$ and a bending strength of 120 MPa, representing an increase of 30, 55 and 70%, respectively, when compared to the nucleated glass. The highest elastic modulus of about 130 GPa was determined for samples treated at 1100 °C. As a preliminary biological evaluation, "in vitro" cytotoxicity tests were realized to determine the cytotoxic level of the materials, using the neutral red uptake method with NCTC clones L929 from the American Type Culture Collection (ATCC) bank. On the other hand, no significant influence of the partial crystallization on cytotoxicity was observed. The results provide support for implant materials based on the $3CaO.P_2O_5$-SiO_2-MgO-system.

*Corresponding author. Tel.: +55 12 31599926; fax: +55 12 31533006.
E-mail address: ju_daguano@yahoo.com.br (J.K.M.F. Daguano).

1751-6161/$ - see front matter © 2012 Elsevier Ltd. All rights reserved.
http://dx.doi.org/10.1016/j.jmbbm.2012.04.024

1. Introduction

Glass-ceramics are inorganic, polycrystalline materials, generally containing a residual glassy phase, obtained by a controlled crystallization of appropriate glasses (Kingery et al., (1975)). This definition indicates that these ceramic materials are not obtained in the usual way, but in a two-step process: first, by melting a glass and conformation into the desired shape and secondly, by the transformation of the glass into a polycrystalline material by nucleation and crystal growth. Depending on the overall composition and heat treatments adopted, it is possible to produce glass-ceramics of different microstructures, having varying amounts of crystal phases, smaller or larger grains, randomly orientated or not, thus resulting in widely varying mechanical properties (Holand and Beall, 2002; Beall, 1992). Glass-ceramics are widely used today in most different environments such as in domestic, structural, thermal, electric and space applications, as well as biomedical (James, 1995).

Of particular interest is the fabrication of biomaterials which may be used in bone restoration. For such biomedical applications, it is important to emphasize some characteristics for glass-ceramics to be applied in bone implants, such as: biocompatibility, and in many cases bioactivity, high flexural strength, elevated fracture toughness and elastic modulus compatible with the human bone (Kokubo et al., 2003). For example, the A/W glass-ceramic Cerabone® (Kokubo, 1993) has been used successfully in cases of vertebral replacement and iliac crest repair. The high strength and high toughness of this glass-ceramic makes it a good load-bearing replacement for cortical bone. By contrast, its elastic modulus is higher than that of cortical bone and its level of bioactivity is insufficient for bonding to soft connective tissues (Hench and West, 1996).

Over the last four decades, researchers have become continuously interested in the development of bioglasses and bioactive glass-ceramics for tissue engineering (Karlsson and Hupa, 2008)(Zhang et al., 2005). Nevertheless, research has tended to focus on bioactivity rather than mechanical properties (Arstila et al., 2005). The first bioactive glass known as Bioglass® 45S5, introduced by Hench (1998) in the beginning of the 1970s, was developed mainly for bone repair. Efforts have therefore been made to develop glass that is less apt to crystallization, but still retaining its bioactivity. Andersson et al. (1992, 1999) extended the investigations by Hench by adding B_2O_3 and Al_2O_3 to the oxide mixture, but theirs studies were concentrated on the in vitro and in vivo bioactivity of glasses controlled by the chemical composition. Moreover, some studies were directed to understand the factors affecting the crystallization of bioactive glasses due to the fact that by adjusting the composition to avoid crystallization special products, such as fibers and porous implants, can be manufactured (Arstila et al. 2007, 2008). Hence, there are only a few studies of the mechanical properties of bioactive glass-ceramics in general and in special for the $3CaO.P_2O_5$-SiO_2-MgO system.

However, this view is challenged by recent data showing new bioactive materials having improved mechanical properties and also better compatibility with human bones are necessary. In this case, fracture strength and Young's modulus (which characterizes the stress–strain response of a brittle material prior to fracture) are fundamental mechanical properties. On the other hand, strength and Young's modulus depend on the microstructure and decrease smoothly and monotonically with increasing porosity (Fan et al., 2012).

In general, the mechanical strength and fracture toughness of glass-ceramics increase when the crystalline phases are incresead (Guazzato et al., 2004; Launey and Ritchie, 2009). Apel et al. (2008) analyzed the crack propagation in commercial glass-ceramics and verified that the crack patterns varied from simple to complex, depending on the amount of the residual glass phase. They stated that the highest crack growth resistance has been observed in materials with the smallest amount of glass phase. In materials with a similar degree of devitrification, other factors such as the grain size, shape and orientation influence the mechanical properties (Launey and Ritchie, 2009; Pinckney and Beall, 2008). For example, elongated grains with an aspect ratio higher than 4, lead to improved fracture toughness by the crack deflection and crack bridging mechanism (Xiang et al., 2007).

In order to improve the mechanical properties of glassy materials, the most commonly used method is to modify the microstructure by partial crystallization (Daguano et al., 2012; Yu et al., 2003; Kansal et al., 2009). On the other hand, partial crystallization of glasses may diminish their bioactivity, even to the point that a bioactive glass turns itself into an inert material (Li et al., 1992). In spite of the fact that glasses within the composition range $1Na_2O$-$2CaO$-$3SiO_2$ and $1.5Na_2O$-$1.5CaO$-$3SiO_2$ may promote enhancement of in vitro bone-like tissue formation in an osteogenic cell culture system, even on fully crystallized glass-ceramics (Moura et al., 2007). In consequence, bioactivity and mechanical properties have to be balanced, depending on the specific use of the glass or glass-ceramic.

The objective of the present study is to determine mechanical properties for glass and glass-ceramics to be used as biomaterials, relating them to the microstructural features such as porosity, crystallinity degree and the type of crystal phases formed. Furthermore, cytotoxicity tests were conducted to evaluate the biocompatibility of these materials.

2. Material and methods

2.1. *Processing*

Bioglass of nominal composition (wt%) 52.75 $Ca_3(PO_4)_2$ 30 SiO_2 17.25 MgO (Oliveira et al., 1997) was prepared from reagent-grade $Ca(H_2PO_4)_2$, $CaCO_3$, SiO_2 and MgO. A batch of 100 g was obtained by mixing the raw materials in ethanol for 240 min, drying at 90 °C for 24 h and passing it through a sieve with openings of 64 μm for deagglomeration.

The glass was prepared according to the conventional melting method in a platinum crucible at 1600 °C. In order to homogenize the melt, a double melting procedure was adopted. The splat cooling method was used to obtain a frit. The frit was remelted at 1600 °C for 4 h in the same platinum crucible. The glass was cast to blocks $15 \times 15 \times 50$ mm in heated metal molds and annealed for 120 min at the

transition temperature (700 °C), previously determined by DSC, and slowly cooled to room temperature.

Samples were further treated at different temperatures 700, 775, 800, 900, 975 and 1100 °C, for 4 h (V700-4, V775-4, V800-4, V900-4, V975-4 and V1100-4), and also cooled down at a rate of 3 °C/min, in order to partially crystallize the glass. These heat-treatments were chosen based on DSC analysis.

2.2. Characterizations

In order to identify the crystalline phases, the heat treated samples were analyzed by high resolution X-ray diffractometry, HRXRD, using a diffractometer with multiple axes, Hubber, Germany. The samples were crushed and sieved to a particle size smaller than 32 μm. The measurements were done in a setup of two coupled concentric circles (ω - 2θ), with a monochromatic X-ray beam of 10 keV ($\lambda = 1.2398$ Å). The powders were put in a cylindrical support of 10 mm diameter and 2 mm depth and were rotated in order to promote randomness of orientation of the crystallographic planes. The diffracted beam was collected by a germanium crystal (200) and a scintillation detector. The powders were analyzed under diffraction angles ranging from 7° to 50°, with a step width of 0.01° and 1 s exposure time per position.

The amount of the crystalline phases (crystallized volume fraction) contained in the glass-ceramic samples was determined according to the procedure used by Krimm and Tobolsky (1951). The percent crystallinity, *IC*, is calculated by the ratio of the crystalline area, A_C, present in the diffractogram of the glass-ceramics and the total area, A_T (A_T=*amorphous*+*crystalline*), present in this diffractogram using the following equation:

$$IC = (A_C/A_T) \times 100 \quad (1)$$

The cross-sections were analyzed using a LEO 1450VP scanning electron microscope. Prior to observation, the sample surface was ground and polished with diamond paste in the sequence 15, 9, 6, 3 and 1 μm. Following this, the microstructure was revealed by chemically etching the polished surface using 0.5 M nitric acid for 30 s. For the SEM investigations, the samples were sputtered with gold.

The real specific mass of the samples was measured by He-pycnometry (AccuPyc 1330, Micromeritics). The apparent density was determined by the immersion method in water using the Archimedes' principle. To measure the apparent porosity, the liquid displacement method was used and water was selected as the displacement liquid (Jiankang et al., 2007). For the purpose of analysis, 10 samples were evaluated from each heat-treatment group.

2.3. Mechanical properties

The modulus of rupture, MOR, was determined in four-point bending tests, according to ASTM C1161-02c (2002), in samples with dimensions of approximately 25 × 2 × 1.5 mm, using a bending device of 20 mm outer and 10 mm inner span, respectively, and using the Universal Testing Machine, MTS 810, 50 N loaded at 0.2 mm/min as rate. For each condition (V700-4, V800-4, V900-4, V975-4 and V1100-4) a minimum of fifteen specimens were tested.

The hardness and the indentation fracture toughness were determined by the Vickers' indentation method, as described in the norms ASTM C1327-08 (2008) and ASTM C1421-10 (2010). The measurements were performed with load of 500 gF with a dwell time of 30 s. A minimum of 21 indentations were performed for each condition.

The elastic modulus E of the glass and the glass-ceramics was determined by the pulse-echo method by measuring the velocities of the longitudinal and transversal ultrasound pulses through the sample. The measurements were performed on a cylindrical specimen with a diameter of approximately 12 mm and 2.5 mm height with polished and parallel surfaces. For the purpose of analysis, 10 samples were evaluated from each heat-treatment group (V700-4, V800-4, V975-4 and V1100-4). The elastic modulus was related with the porosity by an equation proposed by Duckworth-Knudsen:

$$E = E_0 \exp(-bP) \quad (2)$$

This relation is generally used to describe the dependency of the porosity, *P*, on Young modulus, where *E* represents the elastic modulus of the material, E_0 the modulus of the material with zero porosity, *P* the relative porosity and *b* a numerical correction factor equal to 4.1 for *P* smaller than 50% (Ren et al., 2009).

2.3.1. Statistical analysis

Before the statistical analysis, independence, homogeneity and normality of variances of experimental data were tested. After the confirmation of all these requirements, all results were analyzed by ANOVA (one-factor with replication) followed by Tukey's test. For all analyses, 5% was considered the limit of significance and the software SPSS 13.0 for windows (SPSS Inc., Chicago, IL) was used.

2.4. Cytotoxicity procedure

The in vitro biocompatibility of the glass and glass-ceramic samples were evaluated by a cytotoxicity assay described as follows. These tests were performed for the powder samples according to ISO 10993-5 (2009) by the neutral red uptake methodology.

2.4.1. Preparation of extracts

The samples were crushed and sieved until a particle size smaller than 63 μm. The specimens were sterilized in a stove at 160 °C for 60 min. Samples were added to Eagle's minimum medium (MEM) in a proportion of 0.1 g/mL and incubated for 48 h at 37 °C.

2.4.2. Cytotoxicity assays

Cytotoxicity assays were carried out in vitro by using cell culture of mouse connective tissue NCTC clone 929 obtained from American Type Culture Collection (ATCC) by the neutral red uptake methodology. The cells were maintained in MEM (Minimum Eagle's Medium with 10% fetal calf serum, 0.1 mmol dm^{-3} non-essential amino acids and 1.0 mmol dm^{-3} sodium piruvate). Cells were detached with 0.2% trypsin and 0.02% EDTA, and the cellular suspension was adjusted to 3.5×10^5 cells/cm^3.

A 0.2 cm^3 of the cell suspension was seeded in flat-bottomed 96 micro-plate wells (Costar, Cambridge, MA,

USA). The micro-plate was incubated for 24 h at 37 °C in a CO_2 humidified incubator. After this period the medium of the plate was discarded and replaced with 0.2 cm^3 of serially diluted extract of each sample (100, 50, 25, 12.5, and 6.25%). Control of cell culture medium was replaced with complete MEM. In the same micro-plate it was run on positive control (0.02% Phenol solution) and negative control (HDPE). Samples and controls were tested in triplicate test and control groups. The plate was incubated again for 24 h in the same conditions. After 24 h the culture medium and extracts were discarded and replaced with 0.2 cm^3 of 0.005% neutral red diluted in MEM. After 3 h of incubation at 37 °C the dye medium was discarded and the microplate was washed twice with phosphate-saline buffer. Each well received 0.2 cm^3 of 1% acetic acid in 50% ethanol and the optical densities (OD) were measured at 540 nm with an ELISA reader spectrophotometer Sunrise from Tecan. The determination of the cytotoxicity index (IC_{50}), i.e., the concentration of the solution which injures or kills 50% of cell population in the assay, was based on a graph of cell viability percentages (in relation to cell control 100% viability) due to the concentrations of glass or glass-ceramic solutions.

3. Results and discussion

3.1. Phase analysis

The results of the phase analysis by X-ray diffraction of the heat treated samples at different temperatures are shown in Fig. 1. The crystallized volume fraction, *IC%*, of each sample, as determined by Eq. (1), is also indicated.

As show in Fig. 1, the sample treated at 700 °C, V700-4, still shows a diffraction pattern typical for amorphous, glassy materials. It is supposed that the heat treatment was only sufficient for the nucleation of the crystal phases and due to their small amount in the whole sample could not be detected by this method. In the sample treated at 775 °C, the formation of whitlockite can be clearly observed by well-defined peaks in the diffractogram. Samples treated at 800, 900 and 975 °C were quite similar in their phase composition, revealing whitlockite and a not cataloged "transient silicate" as crystalline phases. In sample V1100-4, treated at 1100 °C, the diopside phase instead of the transient silicate has been detected, indicating that a phase transformation took place.

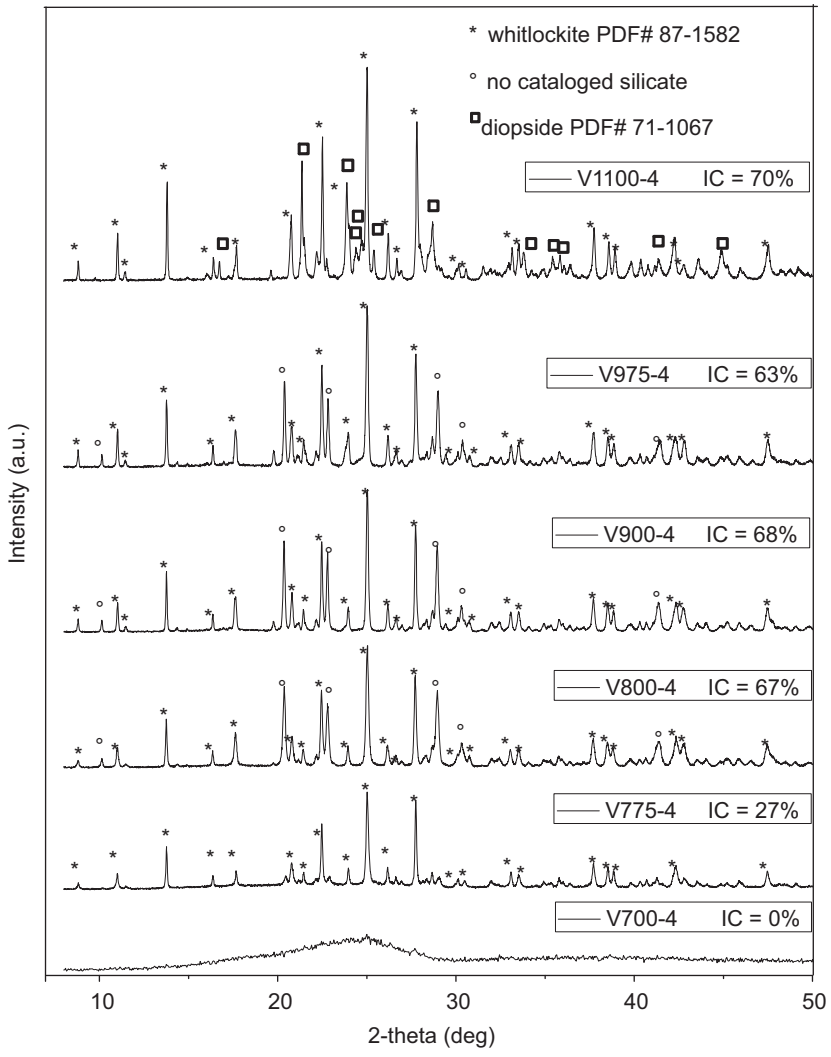

Fig. 1 – X-ray diffractograms of the samples heat treated at 700, 775, 800, 900, 975 and 1100 °C for 4 h. Crystal phases are identified and the degree of crystallinity, *IC*, is also indicated.

Interestingly, this correlation is related to the crystallized volume fraction. It can be seen from the data in Fig. 1 that the higher the temperature is, the more crystallized it is. Sample V775-4 presents an amount of 27% crystal phase, according to the quantitative analysis, while the remaining matrix is still amorphous. The degree of crystallinity (*IC*) increased considerably to 67% by V800-4 and continued to increase, but more minimally to 70% in V1100-4. These findings have important implications for developing bioglass-ceramics which presents improved mechanical properties, as reported by Peitl et al. (2012).

All glass-ceramics studied in this work presented whitlockite as crystal phase, PDF #87–1582, with a substitution of Mg by Ca, $3(Ca,Mg)O.P_2O_5$, independently of the heat treatment temperature. This phase is a tricalcium phosphate with magnesium in solid solution of the composition $Ca_{2,5725}Mg_{0,4275}(PO_4)_2$, also known as β–TCMP.

At temperatures of 800 °C and above a second crystal phase has been detected. Even after detailed and repeated analysis and comparison with existing data bases, JCPDS, it was not possible to identify this phase and therefore has been called a "transient silicate", because apparently this phase transforms into diopside at higher temperatures, see Fig. 1. It is thought that this silicate represents a metastable phase.

A third crystalline phase has been detected only in the sample treated at 1100 °C, being identified as diopside, PDF # 71–1067, $CaMgSi_2O_6$. This phase is the final result of crystallization of the transient silicate found in the samples treated between 800 and 975 °C. This observation is in agreement with the work of Holand and Beall (2002) who reported that when glass-ceramics present metastable phases and are heated up to temperatures sufficiently high that solid state reactions may occur, stable crystal phases develop; in this case the phase formed is diopside.

3.2. *Microstructure*

In Figs. 2 to 5, representative micrographs of the glass and glass-ceramics, obtained under different heat treatments are shown.

The sample treated at 700 °C presents two separated amorphous phases due to an immiscibility gap in the liquid stage, with convoluted structures, known as morulae with a size of 2 to 4 μm, Fig. 2. Oliveira et al. (2000a, 2000b) also confirm the existence of silica rich, amorphous morulae in the system $3CaO–P_2O_5–SiO_2–MgO$. However, at higher temperatures it has been possible to observe that the morulae seem to undergo a disintegration or dissolution process until they disappear at 1100 °C. In Fig. 3 (sample V775-4) three regions may be identified: the amorphous SiO_2 morulae, the

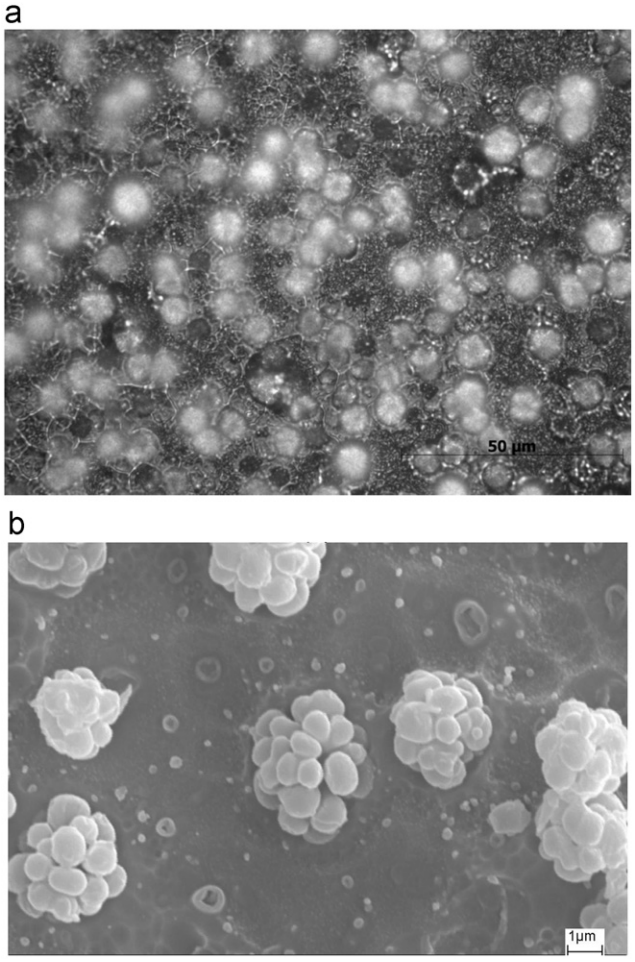

Fig. 2 – Micrographs of the samples heat treated at 700 °C for 4 h. Magnification: x50 (a) and x15000 (b).

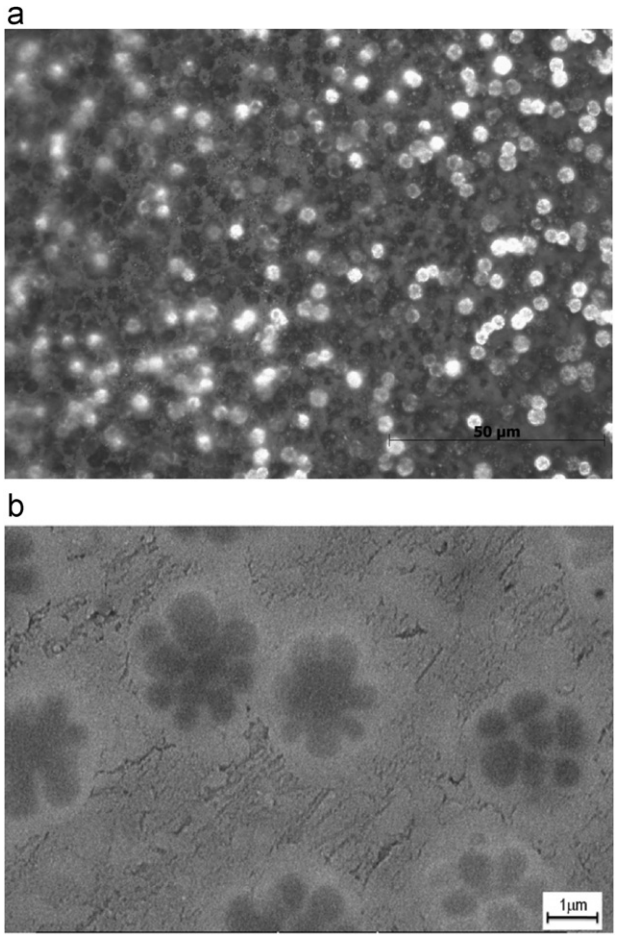

Fig. 3 – Micrographs of the samples heat treated at 775 °C for 4 h. Magnification: x50 (a) and x10000 (b).

residual matrix surrounding the morulae (clearer regions) with phosphor-rich dominions and the silicon-rich residue of the matrix. In this micrograph it has not been possible to identify crystals of whitlockite.

The micrographs of Fig. 4 show that beginning at 800 °C phosphor-rich residual regions of the matrix start to transform into acicular-shaped whitlockite crystals. As the sample surface was chemically etched by 0.5 M nitric acid to reveal the microstructure a large amount of the whitlockite phase has been lixiviated by the acid. We believe that the SiO_2 morulae act as nucleating agent because they form SiO_2 islands surrounded by a phosphor-rich phase depleted of SiO_2, as also reported by Queiroz (2005) for glasses of this system. As shown by the results of the phase analysis, see Fig. 1, at temperatures higher than 800 °C a second phase starts to crystallize. In Fig. 4 the lixiviated acicular phase is whitlockite, the aggregates amorphous silica and the rest is composed of the transient silicate and the reminiscent glass matrix. The whitlockite phase crystallized in very small sub micrometer crystals of high aspect ratio. Furthermore, rounded pores are also observed and the formation of fissures at phase boundaries.

The microstructure of the sample treated at 1100 °C (Fig. 5) represents a microstructure formed at higher temperatures during the crystallization process of glasses from the system $3CaO–P_2O_5–SiO_2–MgO$, characterized by whitlockite crystals embedded in the diopside matrix, by pores formed at the interfaces of phases and still some residual glass phase. With increasing heat treatment temperatures, an increase of the porosity can be noted, which is attributed to the formation of higher density crystalline phases compared to the glass matrix, thus forming voids during transformation. At 1100 °C the amorphous silica has been consumed by the transient silicate and therefore has not been found in the microstructure shown in Fig. 5. Only whitlockite, the glass and diopside are found, besides the presence of pores. The transient silicate is probably converted into the stable phase diopside.

The results of the relative densities are presented in Table 1.

An increase of the specific mass is noted as the temperature of the heat treatment increases, due to the formation of crystalline phases. Sample V700-4, the nucleated glass, presented a specific mass of 2.93 g/cm^3, while sample V975-4 with the crystal phases whitlockite and the transient silicate, besides the residual amorphous glass, showed an increase in the specific mass of 3.5%. The specific mass of sample V1100-4 increased further, presenting a gain of almost 5% in regard to sample V700-4. The crystalline phases whitlockite

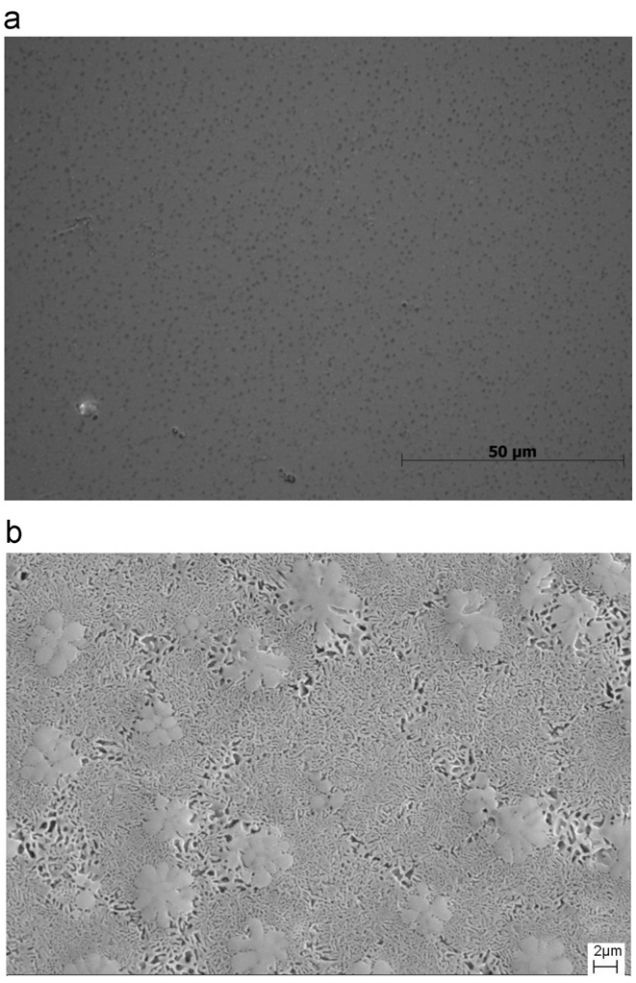

Fig. 4 – Micrographs of the samples heat treated at 975 °C for 4 h. Magnification: x50 (a) and x5000 (b).

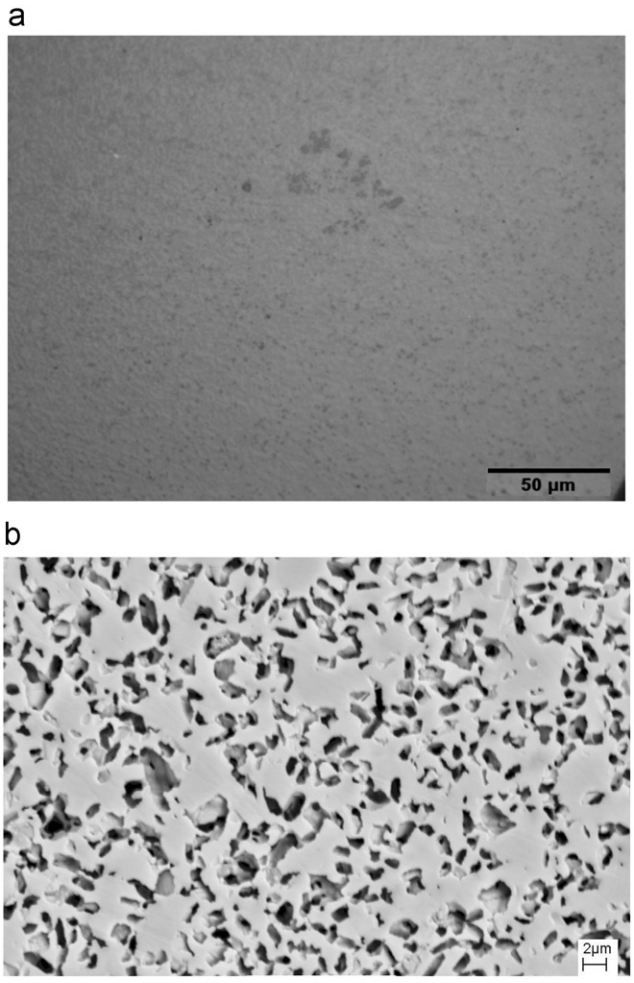

Fig. 5 – Micrographs of the samples heat treated at 1100 °C for 4 h. Magnification: x50 (a) and x5000 (b).

Table 1 – Specific mass, relative density and apparent porosity of the samples treated at 700, 775, 975 or 1100 °C for 4 h.

Heat treatment	Code	ρ_{real} (g/cm^3)	$\rho_{apparent}$ (g/cm^3)	$\rho_{relative}$ (%)	Porosity (%)
700 °C–4 h	V700–4	2.93±0.01	2.87±0.01	98.8±0.3	1.8±0.4
775 °C–4 h	V775–4	2.91±0.01	2.86±0.09	98.3±0.3	2.7±1.2
975 °C–4 h	V975–4	3.04±0.01	2.96±0.01	97.3±0.3	2.3±0.3
1100 °C–4 h	V1100–4	3.08±0.01	2.97±0.12	96.3±2.5	5.4±1.3

Table 2 – Mechanical properties of the heat treated samples.

Sample	Bending Strength (MPa)	Vickers Hardness (GPa)	Indentation Fracture Toughness (MPa.m$^{1/2}$)	Young Modulus*(GPa)	Young Modulus at zero porosity**(GPa)
V700–4	71±4^{a}	4.89±0.15^{a}	1.11±0.12^{a}	85.4±2.4^{a}	92.0
V800–4	105±7^{b}	5.64±0.18^{b}	1.38±0.17^{b}	87.0±1.5^{a}	97.3
V850–4	–	5.79±0.25^{b,c,d}	1.43±0.14^{b}	–	–
V900–4	116±10^{c}	5.92±0.23^{d}	1.49±0.16^{b,c}	–	–
V975–4	119±12^{c}	6.16±0.32^{e}	1.58±0.15^{c}	119.1±3.4^{b}	130.9
V1000–4	–	6.28±0.25^{e}	1.50±0.18^{b}	–	–
V1100–4	69±4^{a}	5.60±0.22^{b,c}	1.45±0.42^{b,c}	129.4±2.7^{c}	161.7

* determined by pulse-echo method.
** by Duckworth–Knudsen Equation.

and diopside present a specific mass of 3.07 and 3.28 g/cm^3, respectively. The formation of these phases causes the increase in specific mass of the glass-ceramics, as described by Holand and Beall (2002). However, relative density of these samples decreases with increasing temperature of the heat treatment and porosity increases. This observation may be related to the formation of pores, in consequence of the crystallization of higher density phases, compared to the glass matrix, Fig. 2 (d). Furthermore, sample V700-4 presents almost 2% of porosity which may be explained by the high viscosity of the molten glass which may have caused the imprisonment of gas bubbles and also by the phase separation due to the immiscibility gap which may lead to pores at the interface.

Karamanov and Pelino (2006, 2008) showed the formation of internal porosity in glass-ceramics of the system diopside—albanite associated to the crystallization of diopside and called this process: "induced crystallization porosity, P_{CR}". The authors attribute the pore formation to the high volume change, ΔV_{Cr}, between the crystals phases formed, such as diopside, from the glass matrix. Porosity is a very important factor for the mechanical properties, as shown in the following results.

3.3. *Mechanical Properties*

Table 2 provides the results obtained from the mechanical properties of samples treated at various temperatures. To compare the effect of partial crystallization on the mechanical properties, an ANOVA (one way) test was used. Treatments followed by distinct letters differ statistically by the Tukey test ($p<0.05$).

Table 2 shows the bending strength of glass and glass-ceramics as a function of the crystallized volume fraction. It is apparent from this table that there is a significant difference between the groups. The average bending strength for samples having a crystalline percentage near 65% is markedly higher than for a glassy sample. An almost 70% increase in the bending strength can be noted comparing the sample treated at 975 °C in relation to the sample treated at 700 °C, which is attributed to the increasing degree of crystallization. However, the sample treated at 1100 °C shows the lowest strength, which might be related to the increased porosity. The fracture surface of these samples shows some porosity as the fracture origin, see Fig. 6.

Moreover, as can be seen from Table 2, there was an increase of hardness associated with crystallized fraction. The hardness increased substantially from sample V700-4 to sample V1000-4, and there was a significant difference between the two groups, as demonstrated by statistical analysis. In contrast, the hardness decreased for a heat-treatment at 1100 °C, due to the higher porosity. Furthermore, it can be observed that the indentation fracture toughness followed the same trend. There was a marked difference between the samples V700-4 and V975-4, on account of the fact that fracture toughness increases 55% from 1.1 to 1.6 MPam$^{1/2}$. A possible explanation for this might be that the crystallization of phases acts as a toughening mechanism causing crack-deflection by the acicular whitlockite phase. This approach can be observed by comparing Figs. 7 and 8.

These results are in agreement with findings of Kashyap et al. (2011) who showed the crack paths in amorphous bioactive glass were straight, yet crack deflections were observed in the crystalline regions. This is likely attributed to different crystallographic orientations of crystals or residual thermal mismatch strains present in the bioglass-ceramic. In addition, the findings of the current study are consistent with those of Peitl et al. (2012) who found that the introduction of crystallinity in bioactive glass of the system P_2O_5–Na_2O–CaO–SiO_2 significantly improves its

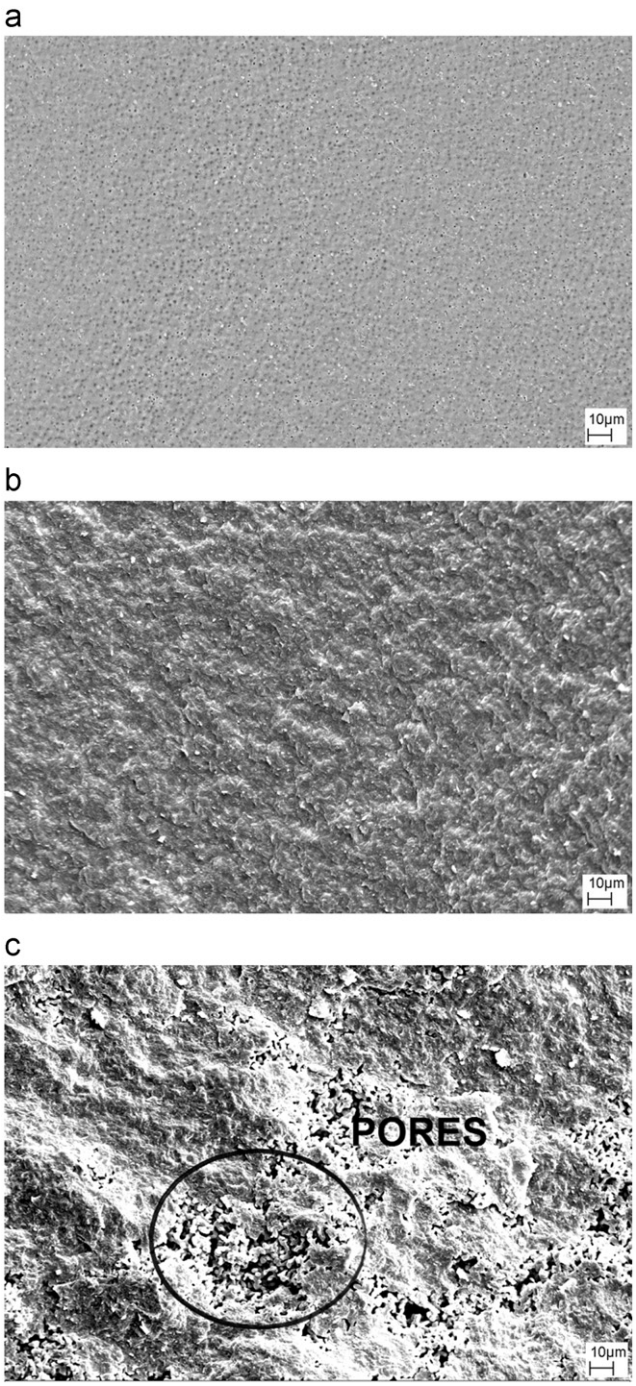

Fig. 6 – Fracture surface of samples (a) V700-4, (b) V975-4 and (c) V1100-4.

mechanical properties. They showed that the improvements in fracture strength and indentation toughness were attributed to crack deflection mechanisms within the material.

Regarding the question of elastic modulus, this study also found that the Young's modulus of the samples tends to increase with increasing degree of crystallization. The initial material, V700-4, presents a modulus of 85 GPa which increases to 120 and 130 GPa for the samples V975-4 and V1100-4, respectively. The ANOVA (one way) showed that these results were statistically different. Considering an exponential decay of the Young's modulus with increasing porosity, the influence of porosity may be eliminated and the modulus of the fully dense materials with zero porosity estimated, see Table 2. Thus, the elastic modulus of the materials without porosity would vary between 92 and 161 GPa, depending on the crystallization degree.

The increase of the Young's modulus is due to the formation of phases with higher modulus than the matrix and is in agreement with literature reports on glass-ceramics based on mica such as the work reported by Vogel (1994). The modulus of sample V700-4 is also in agreement with literature data of silicate based glasses reported by Varshneya (2006).

In general, high elastic moduli suggest a more rigid structure of the material. Therefore, it can be affirmed that the structure composed of diopside and acicular crystals of whitlockite, sample V1100-4, is the most rigid of the samples obtained by the crystallization of glasses from the system $3CaO–P_2O_5–SiO_2–MgO$. This data must be interpreted with caution because Young's modulus is of great importance to select biomaterials with the potential to be used in bone implants due to a phenomenon so-called stress shielding. This occurs when the implant showed elastic modulus higher than that of the bone ($E_{\text{cortical bone}}$~7–30 GPa). In this case, the implant ends up supporting almost all the mechanical load in the region of the prosthesis, decreasing the natural mechanical stress imposed on the bone tissue, and consequently it promoted tissue degeneration (Dai, 2004). It can thus be suggested that this finding is rather disappointing.

3.4. *Cytotoxicity test*

Fig. 9 shows the cytotoxicity evaluation performed by neutral red uptake assay. Positive and negative controls were used to confirm the adequate performance of the test procedure and/or to evaluate the results from a new material, as well as to control cell sensitivity, extraction efficiency, and other test parameters.

The cytotoxic potential can be quantitatively expressed as $IC_{50(\%)}$ (cytotoxicity index), which is easily determined by plotting the percentage of the cell viability in relation to cell control and the concentration of the extract on a graph. $IC_{50(\%)}$ is the concentration of the extract necessary to kill half the cell population, or the extract concentration, which injury or kill half of the cell population, in the assay.

From these curves (Fig. 9), it is possible to observe that the extracts even with high extract concentration do not cause death or injury of the cell population, indicating that these materials presented no cytotoxicity. All studied samples, irrespective of the material's phase, showed the same behavior as negative control. Only positive control showed cytotoxicity presenting cytotoxicity index ($IC_{50\%}$) of about 40% indicating that the extract of positive control in the concentration of 40% injured or killed 50% of cell population in the assay. Besides, the test showed that there is no contamination by the processing in significant amounts to compromise the experiment.

This combination of findings provides some support for the premise that the estimated fracture toughness of V975-4 glass-ceramic is much closer to that of the commercial glass-ceramics Cerabone and Bioverit (Table 3) and is three-fold

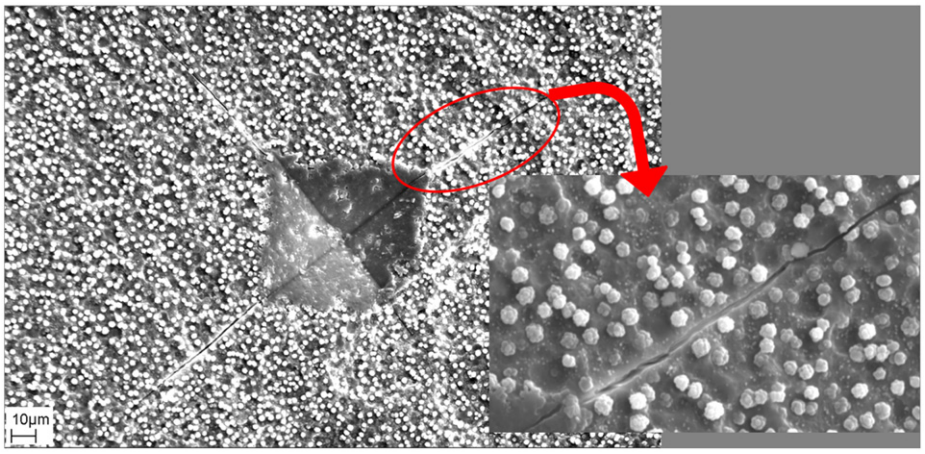

Fig. 7 – Micrograph of a Vickers' indentation mark in sample V700-4 under a load of 19.6 N. The amplified region shows the crack path in more detail.

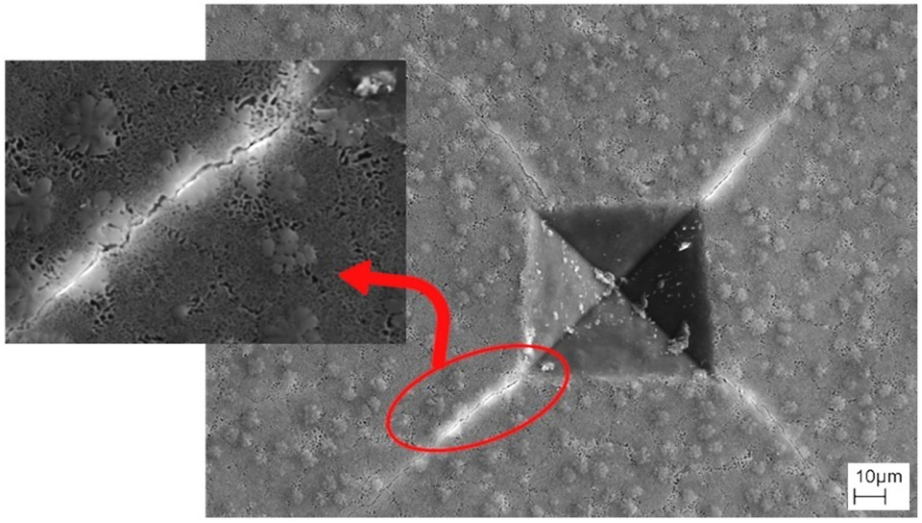

Fig. 8 – Micrograph of a Vickers' indentation mark in sample V975-4 under a load of 19.6 N. The amplified region shows the crack path in more detail.

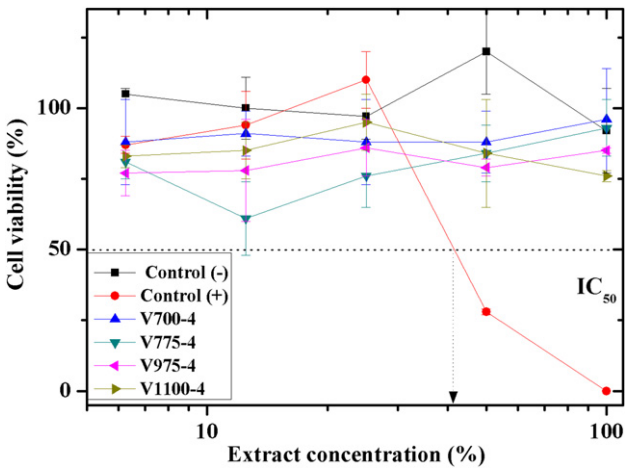

Fig. 9 – Cell viability curves of glass and glass-ceramics studs.

higher than that of the 45S5 Bioglass®. On the other hand, the Young's modulus of V975-4 is significantly higher to that of cortical bone, but is comparable to elastic modulus of the other bioceramics, as Cerabone and Hydroxyapatite. Also, their average fracture strength is among the highest, they are reasonably machinable and their cytotoxicity level is minimal.

4. Conclusions

In summary, this paper has given an account of a new bioglass-ceramics from the system $3CaO–P_2O_5–SiO_2–MgO$ for bone implant application. In this investigation, the aim was to assess the influence of the crystallization process on the mechanical properties and cytotoxicity of the parent glass via different single-stage heat-treatments. The results of this research support the idea that the amount of crystal phases

Table 3 – Mechanical properties of several bioactive materials.

Bioactive materials	*Four-bending Strength (MPa)*	*Vickers Hardness (GPa)*	*Fracture Toughness ($MPa.m^{1/2}$)*	*Young's Modulus (GPa)*
Bioglass®	70	4.5	0.5	50
Cerabone A/W®	215	6.7	2.0	220
Bioverit®	160	6.4	1.2–2.0	90
Biosilicate®	200	6.5	1.0	70
Hydroxyapatite®	40–70	5.9	1.0	120
V975-4 (this work)	120	6.2	1.6	120
Cortical bone	50–150	–	2–12	7–30

formed in this bioactive glass improves hardness, fracture toughness, bending strength and elastic modulus of the materials depending on the heat treatment temperature. In the best case (V975-4) the bending strength increased from 70 to 120 GPa and the indentation fracture toughness from 1.1 to 1.7 $MPa.m^{1/2}$. Finally, a number of important limitations need to be considered. First, this relationship has been observed for temperatures up to 1000 °C. For higher temperatures porosity increases notably, resulting in decreasing mechanical properties. By the end, to obtain an optimized bioactive glass-ceramic, a relatively low elastic modulus is required.

The present study makes several noteworthy contributions to a better understanding of the influence of crystallinity on the mechanical behavior of bioactive glass-ceramics. Since a nontoxic behavior was observed in the cytotoxicity tests, it may be assumed that glasses and glass-ceramics based on the $3CaO.P_2O_5$–SiO_2–MgO-system are viable bioactive materials for clinical applications. Nevertheless, it is recognized that further research should be undertaken in this field.

Acknowledgments

The authors would like to thank Prof. E. D. Zanotto and Prof. C. N. Elias for technical support and B. P. Rodrigues for the help provided during the development of the present work. The authors acknowledge LNLS—Laboratório Nacional de Luz Síncrotron for technical support. Also we give our thanks to FAPESP and CNPq for financial support under the grants 04/04386-1, 07/50681-3, 07/50510-4 and 304544/2010-8, respectively.

REFERENCES

Andersson, Ö.H., Liu, G., Kangasniemi, K., Juhanoja, J., 1992. Evaluation of the acceptance of glass in bone. Journal of Materials Science: Materials in Medicine 3, 145–150.

Andersson, Ö.H., Södergard, A., 1999. Solubility and film formation of phosphate and alumina containing silicate glasses. Journal of Non-Crystalline Solids 246, 9–15.

Apel, E., Deubener, J., Bernard, A., Holand, M., Muller, R., Kappert, H., Rheinberger, V., Holand, W., 2008. Phenomena and mechanisms of crack propagation in glass-ceramics. Journal of Mechanical Behavior of Biomedical Materials I, 313–325.

Arstila, H., Zhang, D., Vedel, E., Hupa, L., Ylänen, H.O., Hupa, M., 2005. Bioactive glass compositions suitable for repeated heat-treatments. Key Engineering Materials 925, 284–286.

Arstila, H., Vedel, E., Hupa, L., Hupa, M., 2007. Factors affecting crystallization of bioactive glasses. Journal of the European Ceramic Society 27, 1543–1546.

Arstila, H., Hupa, L., Karlsson, K.H., Hupa, M., 2008. Influence of heat treatment on crystallization of bioactive glasses. Journal of Non-Crystalline Solids 354, 722–728.

ASTM C1161-02c, 2002. Standard test method for determination for flexural strength of advanced ceramics at ambient temperature. Annual Book of ASTM Standards, USA.

ASTM C1327-08, 2008. Standard Test Method for Vickers Indentation Hardness of Advanced Ceramics. 2008. Annual Book of ASTM Standards, USA.

ASTM C1421-10, 2010. Standard Test Methods for Determination of Fracture Toughness of Advanced Ceramics at Ambient Temperature, Annual Book of ASTM Standards, USA.

Beall, G.H., 1992. Design and properties of Glass-ceramics. Annual Reviews Materials Science 22, 91–119.

Daguano, J.K.M.F., Suzuki, P.A., Strecker, K., Fernandes, M.H.F.V., Santos, C., 2012. Evaluation of the micro-hardness and fracture toughness of amorphous and partially crystallized $3CaO.P_2O_5$–SiO_2–MgO bioglasses. Materials Science and Engineering: A 533, 26–32.

Dai, K., 2004. Rational utilization of the stress shielding effect of implants. In: Poitout, D.G. (Ed.), Biomechanics and biomaterials in orthopedics. Springer-Verlag, Singapore, pp. 208–215.

Fan, X., Case, E.D., Ren, F., Shu, Y., Baumann, M.J., 2012. Part II: Fracture strength and elastic modulus as a function of porosity for hydroxyapatite and other brittle materials. Journal of the Mechanical Behavior of Biomedical Materials 8, 99–110.

Guazzato, M., Albakry, M., Ringer, S.P., Swain, M.V., 2004. Strength, fracture toughness and microstructure of a selection of all-ceramic materials. Part I. Pressable and alumina glass-infiltrated ceramics. Dental Materials 20, 441–448.

Hench, L.L., 1998. A forcast for the future. Biomaterials 19, 1419–1423.

Hench, L.L., West, J.K., 1996. Biological applications of bioactive glasses. Life Chemistry Reports 13, 187–241.

Holand, W., Beall, G.H., 2002. In: Glass-Ceramic Technology. American Ceramic Society, Ohio.

ISO 10993-5, 2009. International Organization for Standardization, Biological Evaluation of Medical Devices. Part 1: Guidance on Selection of Tests.

James, P.F., 1995. Glass ceramics: new composition and uses. Journal of Non-Crystalline Solids 181, 1–15.

Jiankang, H., Dichen, L., Yaxiong, L., Bo, Y., Bingheng, L., Qin., L., 2007. Fabrication and characterization of chitosan/gelatin porous scaffolds with predefined internal microstructures. Polymer 48, 4578–4588.

Karlsson, K.H., Hupa, L., 2008. Thirty-five years of guided tissue engineering. Journal of Non-Crystalline Solids 354, 717–721.

Kansal, I., Goel, A., Tulyaganov, D.U., Ferreira, J.M.F., 2009. Effect of some rare-earth oxides on structure, devitrification and properties of diopside based glasses. Ceramics International 35, 3221–3227.

Karamanov, A., Pelino, M., 2006. Sinter-crystallisation in the diopside–albite system. Part I. Formation of induced crystallisation porosity. Journal of the European Ceramic Society 26, 2511–2517.

Karamanov, A., Pelino, M., 2008. Induced crystallization porosity and properties of sintereds diopside and wollastonite glass-ceramics. Journal of the European Ceramic Society 28, 555–562.

Kashyap, S., Griep, K., Nychka, J.A., 2011. Crystallization kinetics, mineralization and crack propagation in partially crystallized bioactive glass 45S5. Materials Science and Engineering C 31, 762–769.

Kingery, W.D., Bowen, H.K., Uhlmann, D.R., 1975. Phase transformation, Introduction to Ceramics. 2a Edition. Academic Press, INC, New York, pp. 368-375.

Kokubo, T., Kim, H.-M., Kawashita, M., 2003. Novel bioactive materials with different mechanical properties. Biomaterials 24, 2161–2175.

Kokubo, T., 1993. A/W glass-ceramic: processing and properties. In: Hench, L.L., Wilson, J. (Eds.), An Introduction to Bioceramics. World Scientific, Singapore: Ç, pp. 75–88.

Krimm, S., Tobolsky, A.V., 1951. Quantitative X-ray studies of order in amorphous and crystalline polymers. Quantitative X-ray determination of crystallinity in polyethylene. Journal of Polymer Science 7, 57–76.

Launey, M., Ritchie, R.O., 2009. On the fracture toughness of advanced materials. Advance Materials 21, 2103–2110.

Li, P., Yang, Q., Zhang, F., 1992. The effect of residual glassy phase in a bioactive glass-ceramic on the formation of its surface apatite layer in vitro. Journal of Materials Science: Materials in Medicine 3, 452–456.

Moura, J., Teixeira, L.N., Ravagnani, C., Peitl, O., Zanotto, E.D., Beloti, M.M., 2007. In vitro osteogenesis on a highly bioactive glass-ceramic (Biosilicate®). Journal of Biomedical Materials Research 82A, 545–557.

Oliveira, J.M., Fernandes, M.H., Correia, R.N., 1997. Development of a New Glass Ceramic in the System MgO–3CaO.P_2O_5–SiO_2. Bioceramics 5, 7–14.

Oliveira, J.M., Correia, R.N., Fernandes, M.H.V., 2000a. Formation of Convoluted Silica Precipitates during Amorphous Phase Separation in the $Ca_3(PO_4)$–SiO_2–MgO System. Journal of American Ceramics Society 83 (5), 1296–1298.

Oliveira, J.M., Correia, R.N., Fernandes, M.H.V., 2000b. Effect of SiO_2 on amorphous phase separation of CaO–P_2O_5–SiO_2–MgO glasses. Journal of Non-Crystalline Solids 273, 59–63.

Peitl, O., Zanotto, E.D., Serbena, F.C., Hench, L.L., 2012. Compositional and microstructural design of highly bioactive P_2O_5–Na_2O–CaO–SiO_2 glass-ceramics. Acta Biomaterialia 8, 321–332.

Pinckney, L.R., Beall, G.H., 2008. Microstructural evolution in some silicate glass-ceramics: a review. Journal of American Ceramics Society 91 (3), 773–779.

Queiroz, C.M.G.A., 2005. Cristalização de biomateriais vitrocerâmicos e mineralização em meio fisiológico simulado. 2005. 170f. Dissertação (Doutorado em Ciências e Tecnologia dos Materiais)—Departamento de Engenharia Cerâmica e do Vidro, Universidade de Aveiro, Aveiro, 2005.

Ren, F., Case, E.D., Morrison, A., Tafesse, M., Baumann, M.J., 2009. Resonant ultrasound spectroscopy measurement of Young's modulus, shear modulus and Poisson's ratio as a function of porosity for alumina and hydroxyapatite. Philosophical Magazine 89, 1163–1182.

Varshneya, A.K., 2006. Elastic properties and Microhardness of Glass, Fundamentals of Inorganic Glasses 2nd Edition Society of Glass Technology, Sheffield, pp. 187-210.

Vogel, W., 1994. Chapter 10: Crystallization of glasses, Glass Chemistry 2nd ed. Springer-Verlag, Berlin pp.280-362.

Xiang, Q., Liu, Y., Sheng, X., Dan, X., 2007. Preparation of mica-based glass-ceramics with need-like fluorapatite. Dental Materials 23, 251–258.

Yu, B., Liang, K., Gu, S., 2003. Effect of the microstructure on the mechanical properties of CaO–P_2O_5–SiO_2–MgO–F^- glass ceramics. Ceramics International 29, 695–698.

Zhang, D., Vedel, E., Hupa, L., Ylanen, H.O., Hupa, M., 2005. InVitro characterization of Bioactive Glasses. Key Engineering Materials 284-286, 481–484.